NOTICE CONCERNING COPYRIGHT RESTRICTIONS

Mineralogic Interpretation of HyMap Hyperspectral Data, Dixie Valley, Nevada, USA—Initial Results

Dharminder Pal and Gregory D. Nash

Energy & Geoscience Institute
Department of Civil & Environmental Engineering
University of Utah, 423 Wakara Way, Salt Lake City, Utah 84108

Keywords

Dixie Valley, geothermal exploration, HyMap, hyperspectral, mineralogy, Nevada, remote sensing

ABSTRACT

A collaborative effort among U. S. Department of Energy sponsored remote sensing specialists and industry recently culminated in the acquisition of hyperspectral data over a new exploration target in Dixie Valley, Nevada, U. S. A. Related research at the Energy & Geoscience Institute is currently focused on mineralogy mapping at the outcrop level. This will be extended to piedmont and valley fill soils to detect soil mineral anomalies that may be related to buried structures and sinters. Spectral mineral end-members have been extracted and relative mineral abundance maps have been created. Papers and data from this project can be found at http://www5.egi.utah.edu under the geospatial data link.

Introduction

A recent collaborative planning effort among several research organizations including: Caithness Operating Company, LLC, Energy& Geosciences Institute (EGI) at the University of Utah, Lawrence Livermore National Laboratories, The University of California, Santa Cruz, and The University of Nevada, Reno led to the recent acquisition of Integrated Spectronics HyMap™ hyperspectral data over a new exploration target located several kilometers from the current production field in Dixie Valley, Nevada, U. S. A.. This data has 126 bands covering a range from 0.4436 μm to 2.4824 μm with full-width half-maximum values ranging from 0.01360 μm to 0.02190 μm. New information on the mineralogy, lithology, and geologic structure of the area will be gained from the interpretation of the HyMap™ data leading to a better understanding of the geothermal system and possibly new well siting. Current EGI work and this paper is focused on mineralogy mapping, specifically hydroxyl and calcium carbonate bearing minerals, to develop spectral end-members and relative abundance maps to be used in soil mineral anomaly mapping. A similar study led to the identification of soil calcium carbonate and kaolinite anomalies associated with a covered piedmont fault and possibly a buried calcareous sinter near the present Caithness production field (Nash and Johnson, 2002).

Dixie Valley is northeast trending sediment-filled structural trough in west-central Nevada, U.S.A. It is bounded on the northwest by the Stillwater Range and on the southeast by the Clan Alpine Range. Caithness Operating Company, LLC operates a 62 MWe geothermal power plant located in the northwestern quadrant of the valley. Production is related to the Dixie Valley fault zone, which lies near the base of the Stillwater Range. The geothermal system is of the structurally-controlled deep circulation type that is found throughout the Great Basin.

Methodology

To effectively map minerals with hyperspectral data, spectral unmixing must be done to create relative abundance maps. Research Systems ENVI™ image analysis software was used for this purpose as well as other data processing needs thus far in this study. ENVI™ facilitates unmixing through the Spectral Mapping Wizard ™ and through the use of several stand-alone algorithms. Both methods were tested in this study.

Atmospheric Correction

The HyMap™ data underwent atmospheric correction and conversion to apparent reflection during post-processing by Integrated Spectronics before distribution to investigators.

Data Reduction

Before spectral unmixing, data reduction was done. As the spectra in the HyMap™ data set cover a range which, in part, is not necessary to accomplish the current goals of this study, the data reduction was indicated. This facilitates faster processing and reduces the number of variables for statistical analysis. Therefore, the input data were reduced to only those bands falling within the 2.0μm to 2.5 μm range by spectral subsetting. The reduced data set contained bands 98 through 126.

Spectral Mapping Wizard™

The Spectral Mapping Wizard™ was tested first. It leads the user through the ENVI™ hourglass processing flow to automatically find and map spectral end-members from the hyperspectral data.

The following steps performed by the spectral mapping wizard:

1. Minimum noise fraction (MNF);
2. Pixel purity index (PPI);
3. Selection of mineral spectral end-members from the PPI;
4. Mixture tuned matched filtering.

These steps are all completed automatically when using Spectral Mapping Wizard™.

Minimum Noise Fraction: The first step in the Spectral Mapping Wizard™ is the MNF transform (Green et al., 1988; Boardman and Kruse, 1994). MNF is used to determine the inherent dimensionality of image data, to segregate the noise in the data, and to reduce the computational requirement for subsequent processing. The MNF transform uses two-cascaded principal components transformations. The first transformation is based on an estimated noise covariance matrix. This decorrelates and rescales the noise in the data. As a result, the noise has unit variance and no band-to-band correlation. The second transform is a standard principal components transformation of noise-whitened data. The resulting bands of the MNF transformed data are ranked with the largest amount of variance, and useful data, in the first few bands with decreasing data variance and increasing noise in subsequent bands until only noise and no coherent image remains. The noise bands are not used in the subsequent processing. Noise bands can be identified two ways:

1. Eigenvalue plot interpretation—once the MNF process completes, the MNF eigenvalues plot (Figure 1) shows an eignvalue for each MNF transformed band (eigenvalue number). Larger eigenvalues indicate higher data variance in the transformed band. When the eigenvalues approach 1, only noise is left in the transformed band. Therefore, data is selected with eigenvalue numbers with values greater than 1; and
2. Data Dimensionality -- data dimensionally is estimated by using a spatial coherence measure that is represented in a resultant plot showing the wizard's best estimate for the number of non-noise MNF bands (Figure 2).

Pixel Purity Index: The second step is calculation of the PPI (Boardman et al., 1995). The MNF transformed data, minus the noise bands, are used as input to create the PPI image. The PPI image indicates the most spectrally unique pixels. The PPI image is an important product in the hourglass process. The PPI image and the atmospherically corrected apparent reflectance data set can be linked on the computer screen so that, as each potential end-member pixel's spectrum from the PPI image can be viewed and further analyzed. Figure 3 shows Dixie Valley apparent reflectance image overlain on a PPI image along with a kaolinite/smectite mix spectral end-member that was found using the PPI image.

End-member Analysis: The third step is identification of the end-members produced in the PPI image. As mentioned above, the spectrum for each pixel with a high value in the PPI can be visualized using the apparent reflectance image as necessary. Further spectral analysis is facilitated in ENVI™ by the Spectral Analyst™ tools, including the Spectral Angle Mapper (Kruse et al., 1993), spectral feature fitting (Clark et al., 1990; Clark et al., 1991), and binary encoding (Goetz et al., 1988), facilitate statistical matching between an image spectra and a library spectra of a known mineral (Figure 4). However, it is up to the analyst to determine if the matches are correct. The spectral library used in the study was the USGS Digital Spectral Library (Clark et al., 1993). The Spectral Mapping Wizard™ derives end-members automatically.

Mixture tuned matching filtering: In step 4, the end-member spectra selected by the Spectral Mapping Wizard™ are input into the MTMF algorithm (Boardman et al., 1995) to create end-member relative abundance maps. The MTMF results are output to a new dataset that contains double the number of bands as input end-members. These consist of a matched filter (MF) score bands and infeasibility bands. Figure 5 shows an example of an MF and infeasibility band. Where the MF scores are high and the infeasibility scores are low one can have a reasonable expectation that a given pixel will contain a strong component of the mineral used as input.

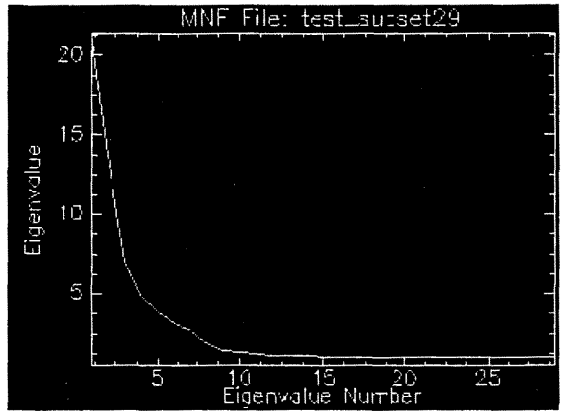

Figure 1. MNF Eigenvalues plot example.

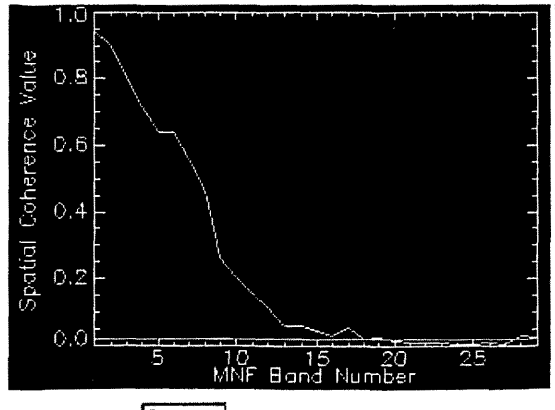

Figure 2. Data dimensionality plot.

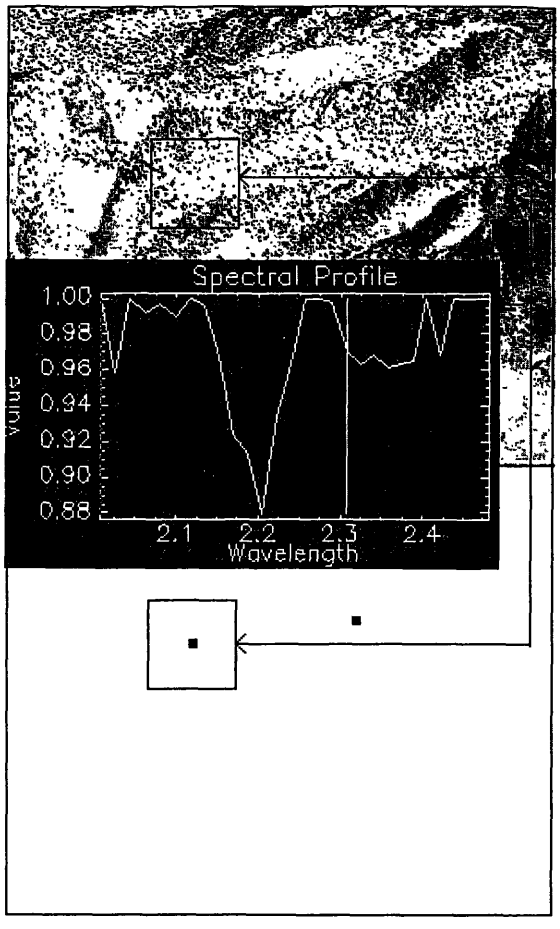

Figure 3. Kaosmectite spectral end-member overlain on a HyMap™ apparent reflection image (top) and a PPI image (bottom). The scattered white pixels in the PPI image are those representing unique spectra.

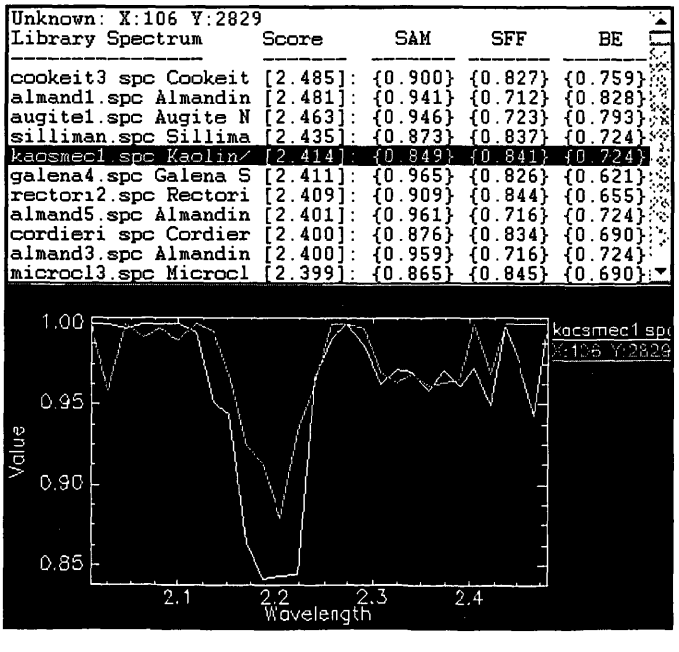

Figure 4. Spectral Analyst spectral correlation results (top) and image spectra stacked with library spectra (bottom) for kaosmectite (kaolinite/ smectite mix).

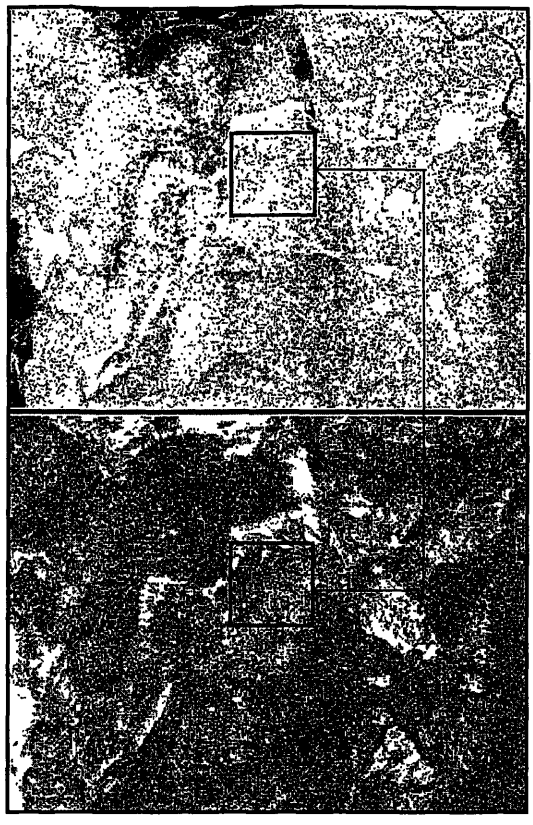

Figure 5. The matched filter score top and infeasibility score on bottom for muscovite.

Results

After running the Spectral Mapping Wizard™ it was determined that some of the results were unreasonable. This was expected. Therefore, the PPI images were examined manually as described above. This allowed refinement in the identification of the end-members. Eight end-members were identified (Figure 6). The end-members were then used as input to the MTMF algorithm to produce new relative mineral abundance images.

After the MTMF is run, scatter plots (Figure 7) are used help identify areas of high probability by allowing a visual comparison of the MF score band with its correlative infeasibility image. Pixels that fall toward the end of the MF axis, with low infeasibility scores, are quickly identified. An area of interest can also be mapped on the scatter plot. This automatically highlights the chosen pixels on the MF image. Maps were produced using this procedure for field use. Ground truth will be done in late May and early June, 2003.

Conclusions

Although this research is still in an early stage, the results thus far look promising. The HyMap™ data's high spatial resolution coupled with its hyperspectral properties may make it the most useful remote sensing data ever acquired over Dixie Valley. Mineral spectral end-members have been identified and relative abundance maps have been created. It will, however, require field work to verify the results, and it is anticipated that the ground truth

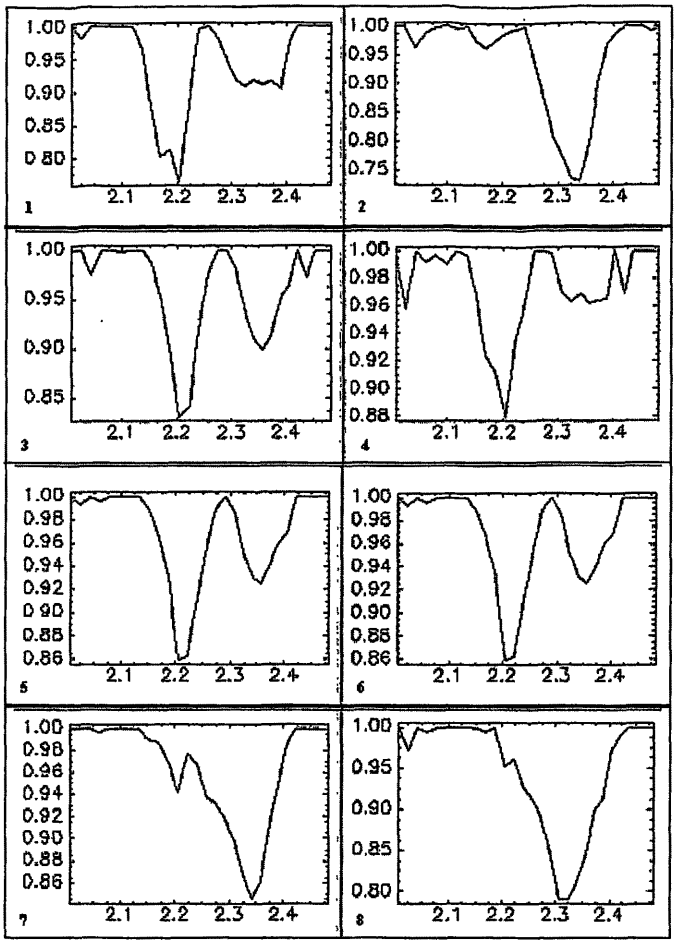

Figure 6. MTMF input end-members. These included the following (1) Kaolinite (2) Calcite, (3) Illite, (4) Kaosmectite, (5) Montomorillonite, (6) Muscovite, (7) Epidote, and (8) Chlorite.

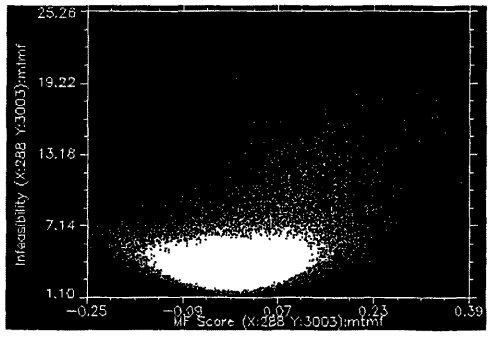

Figure 7. Scatter plot of an MF band and Infeasibility band. The gray area in the lower-right area represents pixel values with a high probability of being an end-member mineral.

will reveal that further analysis is required to improve the relative abundance maps. Papers and data from this project can be found at http://www5.egi.utah.edu under the geospatial data link.

Acknowledgements

This Work is supported by the U.S. Department of Energy under DOE Idaho, Operations Office Contract DE-AC07-001ID13891.

References

Boardman, J. W., and F. A. Kruse, 1994. "Automated Spectral Analysis: A Geologic Example Using AVIRIS Data, North Grapevine Mountains, Nevada." *Proceedings of the Tenth Thematic Conference on Geologic Remote Sensing*, May 9-12, San Antonio, TX., p. I-407 - I-418.

Boardman, J. W., Kruse, F. A., Green, R. O., 1995. "Mapping Target Signatures Via Partial Unmixing of AVIRIS Data." *Summaries: Fifth JPG Airborne Earth Sciences Workshop*, JPL Publications 95-I, v. 1, p. 23-26.

Clark, R.N., A.J. Gallagher, and G.A. Swayze, 1990. "Material Absorption Band Depth Mapping of Imaging Spectrometer Data Using a Complete Band Shape Least-Squares Fit with Library Reference Spectra." *Proceedings of the Second Airborne Visible/Infrared Imaging Spectrometer (AVIRIS) Workshop*, JPL Publication 90-54, p. 176-186.

Clark, R.N., Swayze, G.A., Gallagher, A.J., King, T.V.V., Calvin, W.M., 1993. "The U. S. Geological Survey, Digital Spectral Library: Version 1: 0.2 to 3.0 microns." U.S. Geological Survey *Open File Report 93-592*, 1340 p.

Clark, R.N., G.A. Swayze, A. Gallagher, N. Gorelick, and F. Kruse, 1991. "Mapping with Imaging Spectrometer Data Using the Complete Band Shape Least-Squares Algorithm Simultaneously Fit to Multiple Spectral Features from Multiple Materials." *Proceedings of the Third Airborne Visible/Infrared Imaging Spectrometer (AVIRIS) Workshop*, JPL Publication 91-28, p. 2-3.

Goetz, A. F. H., Vand, G., Solomon, J. E., 1988. "Imaging Spectrometry for Earth Remote Sensing." *Science*, v. 228, p. 1147-1153.

Green, A. A., M. Berman, P. Switzer, and M. D. Craig, 1988. "A Transformation For Ordering Multispectral Data In Terms Of Image Quality With Implications For Noise Removal." *IEEE Transactions on Geoscience and Remote Sensing*, vol. 26, no. 1, p. 65-74.

Kruse, F. A., Letkoff, A. B, Boardman, J. B., Heidebrecht, K. B., Shapiro, A. T., Barloon, P. J., Goetz, A. F. H., 1993. "The spectral Image Processing System (SIPS) – Interactive Visualization and Analysis of Imaging Spectrometer Data." *Remote Sensing of the Environment, Special issue on AVIRIS*, May-June 1993, v. 44, p. 145-163.

Nash, G. D. and G. Johnson, 2002. "Soil Mineralogy Anomaly Detection in Dixie Valley, Nevada Using Hyperspectral Data." *Proceedings: Twenty-Seventh Workshop on Geothermal Reservoir Engineering Stanford University*, Stanford, California, January 28-30, 2001, SGP-TR-171, CD-ROM.